DETERMINATION OF INTERNAL MOISTURE TRANSPORT AND SURFACE EMISSION COEFFICIENTS FOR EASTERN WHITE PINE

Hwanmyeong Yeo†
Assistant Professor

Chang-Deuk Eom
Graduate Research Assistant

Yeonjung Han
Graduate Research Assistant
Department of Forest Sciences
Seoul National University
Seoul, 151-921, Korea

Wook Kang
Research Professor
Division of Forest Resources and Landscape Architecture
Chonnam National University
Gwangju 561-756, Korea

*William B. Smith**†
Professor
Wood Products Engineering
College of Environmental Science and Forestry
State University of New York
Syracuse, NY 13210

(Received October 2007)

Abstract. Moisture movement in eastern white pine wood specimens was evaluated during drying at specific temperature and RH conditions. The objective of this work was to build an appropriate numeric analysis model for predicting moisture profile changes in wood and apply this to the kiln-drying of large cross-section eastern white pine timbers. The internal moisture transport coefficients were dependent on the temperature and average moisture content, and the surface emission coefficients on the water vapor pressure in air adjacent to the surface. The internal moisture transport coefficients decreased with decreasing temperature and internal moisture content. Surface emission coefficients increased with increasing temperature and decreasing surface moisture content.

Keywords: Eastern white pine, mass transfer, kiln-drying, internal moisture transport coefficient, surface emission coefficient, water vapor pressure, coefficient conversion.

INTRODUCTION

Eastern white pine (*Pinus strobus* L.) from the northeastern United States has good color, few dead knots, is easy to machine; and large-dimension white pine timbers have been commonly used for log home construction. Using such green timbers for structural members of log homes, however, often results in such drying defects as excessive in-place shrinkage, distortion, and cracks that occur after construction. This can cause noises, difficulties opening and closing windows and doors, and structural de-

* Corresponding author: wbsmith@esf.edu
† SWST member

formation. Accordingly, with increased demand for use of dried structural timbers has come a need for appropriate kiln-drying schedules and techniques. Development of kiln schedules that could enable rapid drying with minimal defects such as excessively deep and numerous checks requires an understanding of fundamental properties related to mass transfer in wood, including internal moisture transport and surface emission coefficients.

The moisture sorption rate in wood is controlled by two resistances, external resistance from the boundary layer and internal resistance of the wood (Avramidis and Siau 1987). The internal moisture transport coefficient is dependent on the internal resistance, whereas the surface emission coefficient is attributed to the external component. The sorption isotherm graphically depicts equilibrium moisture content (EMC) as a function of RH at a constant temperature (Skaar 1972). Stamm (1964), Skaar (1988), and Siau (1995), in reviews of moisture sorption from a molecular standpoint, conclude that sorption isotherms for all species are characterized by a sigmoid shape. Understanding the relationships among RH, temperature, and EMC of wood is important to most phases of wood processing and to their end uses to optimize processing and minimize the problems associated with shrinking and swelling of wood (Simpson 1980). Yeo and Smith (2005) reported on studies that showed the convective mass transfer coefficient conversion method could be developed by defining appropriately water vapor pressure adjacent to wood surfaces. This study on the drying of white pine timbers investigates moisture movement phenomena through drying experiments that consider the cellular arrangement at the surface and internal regions of wood. Also, a theoretical method able to approximate the unsteady-state external and surface moisture movement at any dynamic environmental situation was analyzed and considered useful in predicting wood moisture content and gradients.

MATERIALS AND METHODS

To determine both internal moisture transport and surface emission coefficients for eastern white pine during drying in the radial or tangential directions, the following clear, straight-grained green specimens were prepared: 80-mm wide (tangential) by 80-mm long (longitudinal) by 20-mm thick (radial), and 80-mm wide (radial) by 80-mm long (longitudinal) by 20-mm thick (tangential). These specimens were obtained from 200-mm-square timbers obtained during a research project on kiln-drying loghome timbers. The decision to select 80 mm for the broad face dimension was specifically to enable the preparation of essentially perfect tangential and radial faces. The four adjacent edge surfaces of each specimen were coated with a commercial wax end sealer to effectively limit moisture movement, forcing moisture movement in the radial direction when drying through tangential faces and in the tangential direction when drying radially. Specific radial and tangential internal moisture transport and surface emission coefficients were determinable from drying experiments with these specimens. Drying was performed in several identical environmental chambers set to four different temperatures—65, 54, 43, and 32°C (nominal values for North American dry bulb set points of 150, 130, 110, and 90°F)—with EMC conditions of 17.3, 13.3, 9.9, and 6.9%, respectively (91–38% RH; Table 1). Temperature and RH were controlled in the chambers to better than ±0.5°C and ±1% RH, respectively. There were five replicates at each condition, and the specific gravity of the specimens averaged 0.34 based on oven-dry mass and green volume. Air velocity was approximately 1 m/s. Average moisture content during drying was calculated from regular weighing of specimens and subsequent oven-drying.

The saturated and partial vapor pressure values in the air adjacent to wood surfaces were obtained from the relationship among dry bulb and wet bulb temperatures, and RH using Kirchoff's and Carrier's equations, respectively (Siau 1995). Target EMC values were determined using the Hailwood and Horrobin coefficient equa-

Table 1. *Test conditions for determining internal moisture transport and surface emission coefficients for eastern white pine.*

Drying time (h)	Dry bulb temperature (°C)	RH (%)	Target EMC (%)
0–209	65	91	17.3
	54	89	17.5
	43	86	17.3
	32	84	17.1
209–327	65	80	13.0
	54	78	13.4
	43	75	13.3
	32	74	13.6
327–421	65	68	9.9
	54	64	10.0
	43	60	9.9
	32	56	9.8
421–479	65	48	6.7
	54	45	6.9
	43	41	7.0
	32	38	7.0

tion obtained from Forest Products Laboratory data over a range of temperature from 0 to 100°C by Simpson (USDA FPL 1999).

RESULTS AND DISCUSSION

The results of drying eastern white pine specimens in the radial or tangential directions are presented as average MC with drying time at each temperature in Fig 1. The points at 209, 327, and 421 h drying time where EMC was reduced from 17.3 to 13.3, 9.9, and then 6.9% (from 91–38% RH) are clearly observable. It is interesting to note that the specimens dried in the radial direction had initial MC substantially lower than the specimens dried tangentially. Although this was not noticed until the experiments were complete, it seems reasonable that the lower MC was from a more rapid initial radial direction drying occurring during specimen preparation.

Figure 2 shows sorption isotherm plots of the target EMC that specimens were exposed to for different temperature and RH conditions using the Hailwood and Horrobin coefficient equation (Simpson 1980; USDA FPL 1999). Actual EMC data measured for the white pine specimens in this study were for the most part within 0.5% MC of the target values, especially at 32 and 43°C. In the 45–80% RH range at the two higher temperatures, the actual EMC values were somewhat lower than the target by approximately 1–2% MC.

Internal Moisture Transport Coefficients (D)

Internal moisture transport coefficients were determined for drying at high MC during the initial high RH drying step at each temperature (Fig 3).

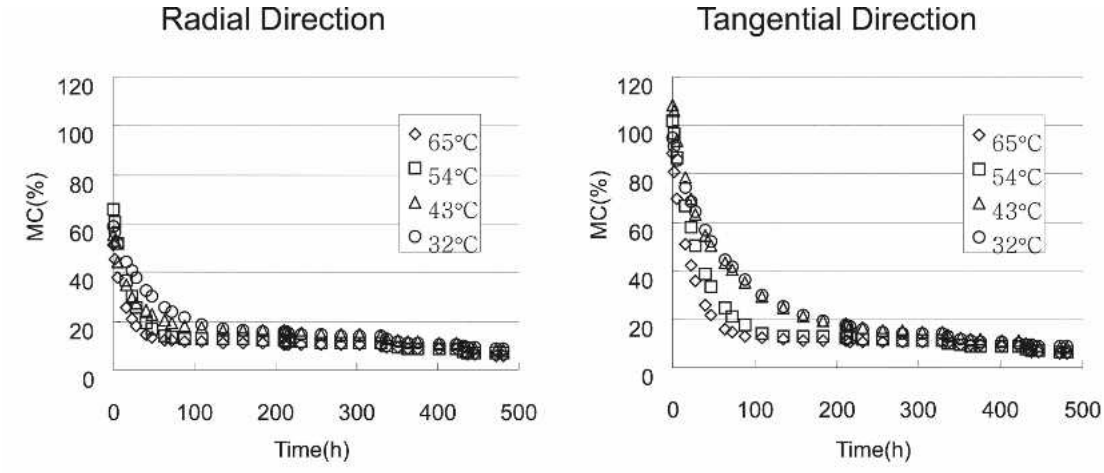

Figure 1. Average moisture content with drying time of specimens dried at four temperatures and four different decreasing EMC.

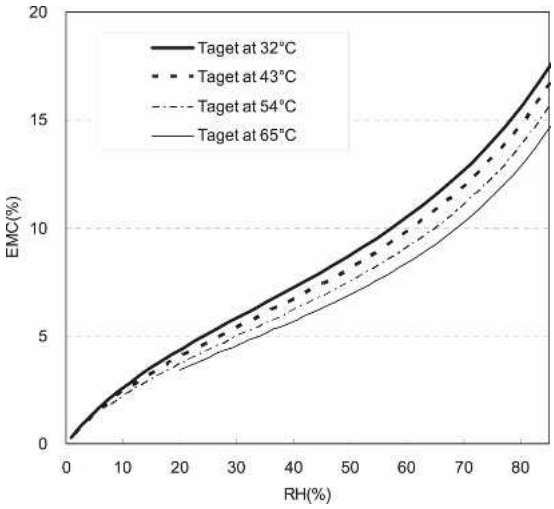

Figure 2. Equilibrium moisture content values at different exposure conditions.

$\overline{E}$ is the fractional change in the average moisture concentration at time t and can be determined as follows (Crank 1956; Yeo 2001):

$$\overline{E} = \frac{\text{AMC} - \text{EMC}}{\text{IMC} - \text{EMC}} \tag{1}$$

$$\overline{E} = \frac{8}{\pi^2} \exp\left(-\frac{\pi^2}{4L^2} \text{D} \cdot \text{t} \right) \tag{2}$$

where D = internal moisture transport coefficient, m^2/s; IMC = initial moisture content, %; AMC = average moisture content, %; EMC = equilibrium moisture content, %; t = time, s; and L = half thickness of specimen, m.

Internal moisture transport coefficients at each of the four drying temperatures were determined by solution of the unsteady-state internal moisture transport equation (Eq 3) derived by the separation of variables method using fractional change in the average moisture concentration (Crank 1956; Yeo 2001):

$$\text{D} = -\frac{4L^2}{\pi^2 \text{t}} \ln\left(\overline{E} \cdot \frac{\pi^2}{8} \right) \tag{3}$$

To determine data values over a broad MC range, a new initial MC was chosen with each measured MC within the ranges shown in Tables 1 and 2. An average of approximately 15 data points were used for each estimation determination of D. Fractional change in the average moisture concentration ($\overline{E}$) was determined using Eq 1. Thereafter, internal moisture transport coefficients could be calculated and compared over various MC ranges. The work in this study is based on the assumption that the external surfaces of a specimen immediately come to equilibrium with the uniform temperature and moisture content of the surroundings (Crank 1956). Table 2 shows average internal moisture transport coefficients of eastern white pine with high, above FSP initial MC, determined at the four drying temperatures with high RH (17.3% EMC). Figure 4 illustrates the internal moisture transport coefficients determined through various MC ranges. The internal moisture transport coefficients are higher in the high temperature condition in which there is much more water activity (Siau 1995) and greater ability of water to move out of the wood. These results also show differences according to cellular orientation with the internal moisture transport coefficient in the radial direction being approximately 30% greater than the tangential. Because the rate of overall initial moisture change depends on the rate of free water movement, this result is probably the result of the contribution of the ray cells.

Siau (1995) presented the transverse internal moisture transport coefficient using the following equation:

$$\text{D}_\text{T} = \frac{1}{(1-a^2)} \cdot \frac{\text{D}_\text{BT} \cdot \text{D}_\text{V}}{\text{D}_\text{BT} + \text{D}_\text{V}(1-a)} \text{ at } \text{M} < \text{Mf} \tag{4}$$

where D_T = transverse bound water internal moisture transport coefficient of wood, m^2/s; D_BT = transverse bound water internal moisture transport coefficient of the cell wall, m^2/s; D_V = water-vapor internal moisture transport coefficient of air in the lumens based on the concentration of bound water in the cell wall, m^2/s; Mf = fiber saturation point; and a = diameter of lumens. Values for D_T calculated from this equation are 1.66×10^{-9} to 4.33×10^{-10}

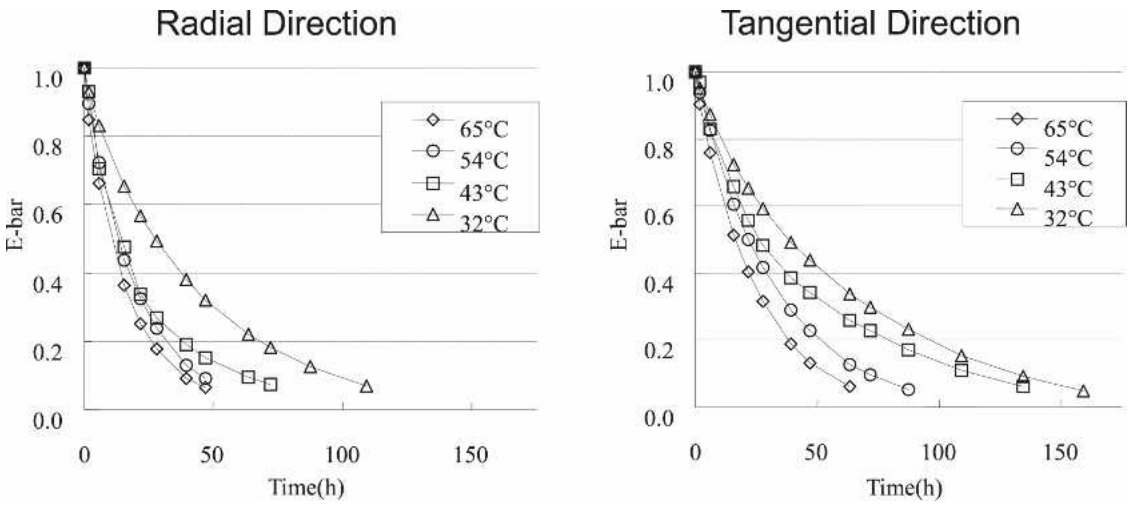

Figure 3. Fractional change in the average moisture concentration (E = E–bar) during radial and tangential direction only drying at four different conditions: 65, 54, 43, and 32°C at 17.3% EMC.

Table 2. *Average radial and tangential internal moisture transport coefficients of eastern white pine with high initial MC determined at four temperatures with high RH (17.3% EMC).*

Drying condition		Radial direction		Tangential direction	
Temperature (°C)	RH (%)	MC (%)	D (m^2/s)	MC (%)	D (m^2/s)
65	91	51–10.6	6.1E-10	88–10.9	5.6E-10
54	89	66–11.9	5.8E-10	102–12.3	4.3E-10
43	86	54–16.0	4.7E-10	106–16.0	3.0E-10
32	84	59–15.6	3.2E-10	95–17.4	2.5E-10

m^2/s at 65°C and 25–11% MC; 1.12×10^{-9} to 3.12×10^{-10} m^2/s at 54°C and 25–12% MC; 7.40×10^{-10} to 3.04×10^{-10} m^2/s at 43°C and 25–16% MC; and 4.74×10^{-10} to 1.90×10^{-10} m^2/s at 32°C and 25–16% MC. The internal moisture transport coefficients calculated for white pine, presented in Table 2 and Fig 4, are comparable to these values. These results validate use of the transverse internal moisture transport coefficient presented by Siau (1995) to approximate the unsteady-state internal moisture movement in wood. Of course, the internal moisture transport coefficient presented by Siau (1995) does not separate or explain differences between radial and tangential rates of internal moisture movement. For wood species having large differences in internal moisture movement rate in each orientation, there exists a need to develop appropriate new models that separately take into account internal moisture transport coefficients obtained in each direction.

Table 3 presents average radial and tangential internal moisture transport coefficients determined for eastern white pine with low initial MC (below FSP) with three decreasing target EMC conditions at the four temperatures. These results show that the internal moisture transport coefficient increases with temperature and exposure to lower RH. It is particularly interesting to note that although the internal moisture transport coefficients are significantly different in the tangential and radial directions when the initial moisture content is above the fiber saturation point (Table 2), with dry wood, the differences between the radial and tangential directions are small (Table 3). This indicates that water vapor diffusion (the phenomenon of moisture condensation and evaporation as water moves through cell walls and lumens) and bound water diffusion in the cell wall are not particularly related to the presence of permeable ray cells.

Surface Emission Coefficients

From the data in Table 3 it can be seen that internal moisture transport coefficients deter-

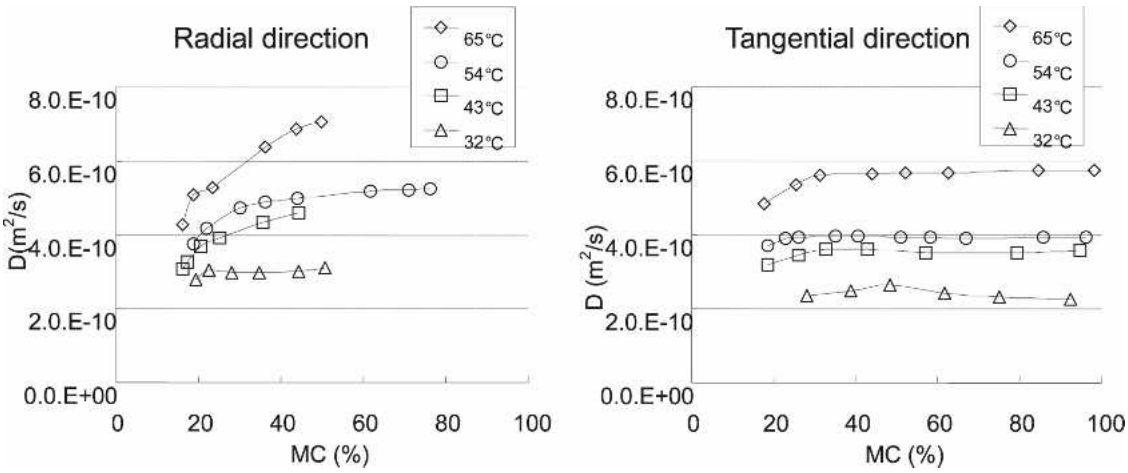

Figure 4. Radial and tangential internal moisture transport coefficients determined for eastern white pine while drying from high initial MC at four temperatures.

Table 3. *Average radial and tangential internal moisture transport coefficients of eastern white pine with low initial MC determined at 13.3, 9.9, and 6.9% target EMC at four temperatures.*

Drying condition		Radial direction		Tangential direction	
Temperature (°C)	RH (%)	MC (%)	D (m^2/s)	MC (%)	D (m^2/s)
65	80	11.0–10.2	4.0E-10	11.0–10.5	3.4E-10
	68	10.2–8.7	5.0E-10	10.5–8.9	5.9E-10
	48	8.7–6.0	1.6E-09	8.9–6.0	1.7E-09
54	78	12.0–11.1	3.8E-10	12.0–11.2	4.2E-10
	64	11.1–8.7	5.9E-10	11.2–8.6	6.2E-10
	45	8.7–6.8	1.2E-09	8.6–6.6	1.2E-09
43	75	15.0–13.0	3.5E-10	16.8–13.5	3.2E-10
	60	13.0–10.0	5.2E-10	13.5–10.1	5.3E-10
	41	10.0–7.3	8.1E-10	10.1–7.3	8.4E-09
32	74	16.0–13.8	3.6E-10	17.0–14.0	4.2E-10
	56	13.8–10.3	4.7E-10	14.0–10.1	5.0E-10
	38	10.3–8.8	6.5E-10	10.1–8.5	6.4E-09

mined at severe drying conditions (high temperature and low RH) are larger than at mild conditions of low temperature and high RH. When analyzing the moisture to be reduced during drying, this study did not distinguish between the quantity of internal moisture that moves to the surface and the quantity of moisture that evaporates from the surface to the surrounding air. Although we could analogize the apparent drying rate to use these results at given temperature and RH conditions, there is still a need to evaluate the more correct moisture movement in wood of various dimensions and initial moisture contents. A primary goal of this study, therefore, was to distinguish external from internal drying resistance.

The surface emission coefficient, which is represented as a reciprocal of external resistance, including surface resistance, can be converted from the convective mass transfer coefficient (Siau 1995). Convective mass transfer coefficients based on the potential of water vapor pressure were experimentally determined by the Hart (1977) method as:

$$h_p = \frac{J}{(p_s - p_e)} \quad (5)$$

where h_p = convective mass transfer coefficient based on the potential of water vapor pressure, kg/m^{2}s Pa; J = moisture flux from the surface of wet wood to air, kg/m^{2}s; p_s = water vapor pressure in air adjacent to the wood surface, Pa; and p_e = water vapor pressure in ambient air at the dry bulb temperature, Pa.

When calculating h_p, the saturated vapor pressures at wet bulb ($p_{o,wet}$) temperature were used as water vapor pressure in air adjacent to the wood surface (p_s). At 65, 54, 43, and 32°C, the average initial moisture fluxes leaving from the tangential surface of wood (radial internal moisture movement) were 4.49×10^{-5}, 3.90×10^{-5}, 2.74×10^{-5}, and 2.21×10^{-5} kg/m^{2}s; and the fluxes leaving from the radial surface of wood (tangential internal moisture movement) were 5.20×10^{-5}, 3.71×10^{-5}, 2.56×10^{-5}, and 2.47×10^{-5} kg/m^{2}s, respectively. As previously shown, in the initial drying stage, moisture fluxes leaving from the surfaces of the wet specimens for each directional surface were similar to each other.

Using Eq 5 with the initial moisture fluxes (J), the saturated vapor pressures at the wet bulb temperature ($p_{o,wet}$), and partial vapor pressure of water in ambient air (p_e) at 65°C/91% RH, 54°C/89% RH, 43°C/86% RH, and 32°C/84% RH, h_p values were calculated.

The h_p values for tangential surface (radial internal moisture movement) at 65°C/91% RH, 54°C/89% RH, 43°C/86% RH, and 32°C/84% RH were 4.19×10^{-7}, 2.97×10^{-7}, 1.81×10^{-7}, and 1.42×10^{-7} kg/m^{2}s Pa, respectively. The h_p values for radial surface (tangential internal moisture movement) at the four different conditions were 4.85×10^{-7}, 2.83×10^{-7}, 1.69×10^{-7}, and 1.59×10^{-7} kg/m^{2}s Pa, respectively.

Also, the convective mass transfer coefficients based on the moisture concentration in air were determined by boundary layer theory as:

$$h_{H20,air} = \frac{0.66 D_{H2O,air}\, Re^{0.5}\, Sc^{1/3}}{L_s} \text{ for laminar flow,} \quad (6)$$

where, $h_{H2O,air}$ = convective mass transfer coefficient averaged over the length L_s, m/s; $D_{H2O,air}$ = diffusion coefficient of water vapor in air, m^2/s; $D_{H2O,air} = 2.2 \cdot 10^{-5}(1.013 \cdot 10^5/P) \cdot (T/273)^{1.75}$ (Dushman's equation, cited by Siau 1995); Re = Reynolds number = $L_s \cdot v \cdot \rho_a/\mu$; Sc = Schmidt number = $\mu/\rho_a D_{H2O,air}$; L_s = length of surface along which convection occurs, m; P = total pressure of air and water vapor, Pa; T = Kelvin temperature of air, K; v = air velocity, m/s; ρ_a = density of air, kg/m^3; and μ = dynamic viscosity of air, Pa · s.

At 65°C, $h_{H2O,air}$ was 1.435×10^{-2} m/s;

$$D_{H2O,air} = 2.2 \cdot 10^{-5}\left(\frac{1.013 \cdot 10^5}{1.013 \cdot 10^5}\right) \cdot \left(\frac{338}{273}\right)^{1.75} = 3.197 \times 10^{-5}\ \text{m}^2/\text{s}; \quad (6\text{–}1)$$

$$\text{Reynolds number (Re)} = \frac{L_s \cdot \nu \cdot \rho_a}{\mu} = \frac{0.08\ \text{m} \cdot 1\ \text{m/s} \cdot 1.042\ \text{kg/m}^3}{0.00002022\ \text{Pa} \cdot \text{s}} = 4123; \quad (6\text{–}2)$$

$$\text{Schmidt number (Sc)} = \frac{\mu}{\rho_a D_{H2O,air}} = \frac{0.00002022\ \text{Pa} \cdot \text{s}}{1.042\ \text{kg/m}^3 \cdot 3.197 \times 10^{-5}\ \text{m}^2/\text{s}} = 0.605; \quad (6\text{–}3)$$

$$h_{H2O,air} \text{ at } 65°\text{C} = \frac{0.66 \cdot D_{H2O,air} \cdot Re^{0.5} \cdot Sc^{1/3}}{L_s} = \frac{0.66 \cdot 3.197 \times 10^{-5}\ \text{m}^2/\text{s} \cdot 4123^{1/2} \cdot 0.605^{1/3}}{0.08\ \text{m}} = 1.435 \times 10^{-2}\ \text{m/s}; \quad (6\text{–}4)$$

and $h_{H2O,air}$ at 54°C, 43°C, and 32°C were 1.394×10^{-2}, 1.353×10^{-2}, and 1.312×10^{-2} m/s, respectively.

Using the conversion method presented by Yeo and Smith (2005), h_p and $h_{H2O,air}$ values were converted to surface emission coefficients (S or $h_{H2O,wood}$). The surface emission coefficients may be expressed in terms of any other by converting the potential as follows:

$$S = h_{H2O,wood} = h_p \cdot \frac{(p_s - p_e)}{(C_{s,wood} - C_{e,wood})} = h_p \cdot \frac{p_s - p_e}{G_{SMC} \cdot \rho_W \cdot \frac{SMC}{100} - G_{EMC} \cdot \rho_W \cdot \frac{EMC}{100}} \quad (7\text{–}1)$$

$$S = h_{H2O,wood} = h_{H2O,air} \cdot \frac{(C_{s,air} - C_{e,air})}{(C_{s,wood} - C_{e,wood})} = h_{H2O,air} \cdot \frac{\frac{M_{H2O} \times p_s}{R \cdot T_s} - \frac{M_{H2O} \times p_e}{R \cdot T_{dry}}}{G_{SMC} \cdot \rho_W \cdot \frac{SMC}{100} - G_{EMC} \cdot \rho_W \cdot \frac{EMC}{100}} \quad (7\text{–}2)$$

where $S = h_{H2O,wood}$ = surface emission coefficient, m/s; $C_{s,wood}$ = moisture concentration in wood at surface, kg/m^3; $C_{e,wood}$ = moisture concentration in wood in equilibrium with air, kg/m^3; and p_s = water vapor pressure in air adjacent to surface of wood, Pa;

$$p_s = p_{o,wet} - \left(\frac{p_{o,wet} - p_e}{100 - RH_e}\right) \cdot (100 - RH_s) = p_{o,wet} - \left(\frac{p_{o,wet} - p_{o,dry} \cdot \left(\frac{RH_e}{100}\right)}{100 - RH_e}\right) \cdot (100 - RH_s) \quad (7\text{–}3)$$

$p_{o,wet}$ = saturated water vapor pressure at wet bulb temperature, Pa; $p_{o,dry}$ = saturated water vapor pressure at dry bulb temperature, Pa; p_e = water vapor pressure in ambient air (= $p_{o,dry} \cdot RH_e/100$), Pa; RH_s, and RH_e = relative humidity of air adjacent to surface of wood and ambient air, %; ρ_w = density of water, kg/m^3; SMC and EMC = surface and equilibrium moisture content, %; G_{SMC} and G_{EMC} = specific gravities of wood based on oven-dry weight and volume at SMC and EMC; $C_{s,air}$ = moisture concentration in air adjacent to wood surfaces, kg/m^3; $C_{e,air}$ = moisture concentration in ambient air, kg/m^3; M_{H2O} = water molecular weight, 18 kg/kmol; R = universal gas constant, 8314 m^{3}Pa/kmol K; T_s = surface temperature, K; and T_{dry} = dry bulb temperature, K.

Figure 5 illustrates surface emission coefficients determined at high initial moisture content at four temperature and RH conditions. Because the RH_e, $P_{o,wet}$, and $P_{o,dry}$ were known values, P_s at any RH_s conditions could be determined using Eq 7–3. Using the P_s value and EMC, the surface emission coefficient (S) converted from h_p and that coefficient converted from $h_{H2O,air}$ could be determined at any SMC conditions by Eq 7–1 and 7–2.

These results show that the higher the temperature and the lower the surface moisture content, the higher the surface emission coefficient. In-

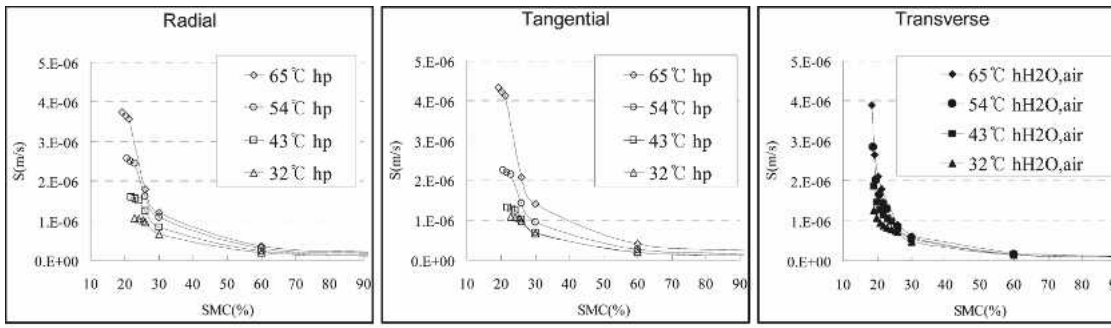

Figure 5. Surface emission coefficients in the radial (a) and tangential (b) directions converted from convective mass transfer coefficient (h_p) determined with measured moisture fluxes and water vapor pressures in air adjacent to surface of wood and surface emission coefficients in the transverse direction (c) converted from convective mass transfer coefficients ($h_{H2O,air}$) calculated by boundary layer theory at various surface moisture contents.

terestingly, there was no particular difference between the coefficients in radial and tangential directions. These results prove surface emission coefficients to be strongly dependent on the SMC and air temperature, and not moisture movement direction.

Also illustrated in Fig 5 is that the surface emission coefficients converted from convective mass transfer coefficient (h_p) determined with measured moisture flux and water vapor pressure in air adjacent to the surface of wood were close to the values converted from convective mass transfer coefficients ($h_{H2O,air}$) calculated by boundary layer theory. This proves that the surface emission coefficients converted from convective mass transfer coefficients calculated by boundary layer theory can be used to approximate the unsteady-state external and surface moisture movement in wood at any dynamic temperature and RH environmental situation.

CONCLUSIONS

Internal moisture transport and surface emission coefficients in both radial and tangential directions for eastern white pine were determined and evaluated during unsteady-state drying conditions. The internal moisture transport coefficients were found to be dependent on the temperature and average moisture content in wood. The transverse internal moisture transport coefficients presented by Siau (1995) were quite comparable to the internal moisture transport coefficients determined in the unsteady-state drying conditions of this study, substantiating that Siau's diffusion coefficients can be used to approximate the unsteady-state internal moisture movement in wood.

The surface emission coefficients were dependent on the water vapor pressure in air adjacent to the wood surface. The surface emission coefficients converted from convective mass transfer coefficients, determined with measured moisture flux and water vapor pressure in air adjacent to the surface of wood, were close to the values converted from convective mass transfer coefficients theoretically calculated by boundary layer theory. This proves that the surface emission coefficients converted from convective mass transfer coefficients calculated by boundary layer theory can be used to approximate the unsteady-state external and surface moisture movement at any dynamic environmental situation. It is anticipated that through use of both internal moisture transport and surface emission coefficient values, actual MC profiles in white pine timbers could be predicted at any drying condition and time.

REFERENCES

Avramidis S, Siau JF (1987) An investigation of the external and internal resistance to moisture diffusion in wood. Wood Sci Technol 21:249–256.

Crank J (1956) Mathematics of diffusion. Clarendon Press, Oxford, UK. 414 pp.

Hart CA (1977) Effective surface moisture content of wood during sorption. Wood Sci 9(4):194–201.

Siau JF (1995) Wood: Influence of moisture on physical properties. Dept. of Wood Sci. and Forest Prod., Virginia Tech, Blacksburg, VA. 227 pp.

Simpson W (1980) Sorption theories applied to wood. Wood Fiber Sci 12:183–195.

Skaar C (1972) Water in wood. Syracuse University Press, New York, NY. 218 pp.

——— (1988) Wood–water relations. Springer-Verlag, New York, NY. 283 pp.

Stamm AJ (1964) Wood and cellulose science. The Roland Press, New York, NY. 549 pp.

USDA FPL (1999) Wood handbook: Wood as an engineering material, FPL GPR–113. Forest Products Society, Madison, WI.

Yeo H (2001) Evaluation of mass transfer in wood utilizing a colormetric technique and numerical analysis. PhD Thesis, SUNY-ESF, Syracuse, NY. 200 pp.

———, Smith WB (2005) Development of a convective mass transfer coefficient conversion method. Wood Fiber Sci 37(1):3–13.